Struct Chem (2016) 27:1291–1302
DOI 10.1007/s11224-016-0779-9

ORIGINAL RESEARCH

A comprehensive computational analysis of cathinone and its metabolites using quantum mechanical approaches and docking studies

Wojciech Kolodziejczyk[1,2] · Supratik Kar[2] · Glake A. Hill[2] · Jerzy Leszczynski[2]

Received: 3 May 2016 / Accepted: 22 May 2016 / Published online: 2 June 2016

Abstract Conformers of the psychoactive compound of the *Khat* plant cathinone along with its amino alcohol metabolites norephedrine and norpseudoephedrine have been calculated using DFT (M062X/B3LYP) and MP2 levels of theory for gas and solution phases. Gas-phase studies revealed that cathinone has two, norephedrine has four and norpseudoephedrine has three low-energy conformations with all conformers connected by rotational transition states. To understand the solvent effect to the energetic profiles of the studied species, the conductor-like screening model is employed within aqueous medium. It explains lowering of energy of all studied conformers in solution. The molecular electrostatic potential surface data for each molecule revealed likely reaction sites for the studied molecules. The computed IR spectra for cathinone and its metabolites have been compared with experimental data and rotational transition states connecting all conformers have been reported. The natural bond orbital analyses for only ligands and separately for their complexes with amino acid residues in protein pockets from the docking results are also performed to corroborate the results obtained from the MP2 and DFT calculations. The comprehensive computational study explore important amino acid residues and stabilizing energy of the studied molecules with the interacting proteins along with the reason behind the difference in potency for cathinone's metabolites.

Keywords Cathinone · DFT · Docking · Gaussian · MP2 · Molecular electrostatic potential · NBO · Norephedrine · Norpseudoephedrine

Introduction

Cathinone, is a naturally occurring psychoactive substance obtained from the leaves of Khat (*Catha edulis*), an evergreen plant that grows at high attitudes in East Africa and Arabian Peninsula [1]. Cathinone is chemically β-keto-amphetamine, which can easily permeate the blood brain barrier (BBB) layer, causing sympathomimetic and psychostimulant actions by acting as a central nervous system (CNS) stimulant by promoting the release of monoamine neurotransmitters and likely inhibiting their uptake [2]. In recent years, cathinone and its derivatives are appeared in the illicit drugs market and these materials can be easily purchased from the internet at low cost [3]. Cathinone users report increased level of energy, a sensation of elation, and an enhanced imaginative ability similar to the effect of amphetamine [4]. Along with cathinone, other less potent stimulant substances are also present in khat leaves, namely norephedrine and norpseudoephedrine (cathinone) [5]. Taking into account the structural and pharmacological properties of amphetamine and cathinone, it can be concluded that they should act similarly by inducing dopamine releases from central dopaminergic nerve terminals, thus increasing the activity of dopaminergic pathways [6, 7].

Norephedrine or phenylpropanolamine (PPA) is a synthetic form of the ephedrine alkaloid that occurs naturally

Electronic supplementary material The online version of this article (doi:10.1007/s11224-016-0779-9) contains supplementary material, which is available to authorized users.

✉ Wojciech Kolodziejczyk
dziecial@icnanotox.org

[1] Department of Physical Chemistry, Wroclaw Medical University, ul. Borowska 211A, 50-556 Wroclaw, Poland

[2] Interdisciplinary Center for Nanotoxicity, Department of Chemistry and Biochemistry, Jackson State University, 17910, 1400 J.R. Lynch Street, Jackson 39217, MS, USA

in plants of the genus Ephedra and one of the major metabolite of cathinone. It is generally used as a bronchodilator and also used as part of appetite suppressants. But, after a number of reported adverse effects (headache, intracranial, elevated blood pressure to cardiopulmonary arrest and even death), the FDA issued a public health warning to consumers; thus, PPA is no longer sold in USA without a prescription. In Canada, this drug ingredient was withdrawn from the market on 2001 [8]. However, in many countries PPA is still available, especially as a component of pharmaceutical products for the treatment of cold. Despite the extensive information about PPA toxicity, amazingly the number of scientific research is very scarce. Again, another metabolites of cathinone is L-norpseudoephedrine also referred as (−)-*threo*-β-hydroxyamphetamine, which is a psychostimulant drug of the amphetamine family. Similar to cathinone, L-norpseudoephedrine acts as a releasing agent of norepinephrine and to a lesser extent of dopamine [9].

Because of amphetamine-like effects and its resultant high abuse potential, cathinone and its metabolites were assigned Schedule I status by the US Drug Enforcement Administration (DEA) in 1993 and Class B status under the UK Misuse of Drugs Act in 1998 [10]. According to the American Association of Poison Control Centers report, 304 human exposure to bath salts calls across the country in 2010 and 6138 in 2011, representing a 2019 % increase within a 1-year span in the United States [11]. Drug Enforcement Administration (DEA) National Forensic Laboratory Information System also received an increase in reports of seizures due to cathinone and its derivatives, receiving 14 reports in 2009 from 8 states to 290 reports from 21 states in 2010 [10]. The patterns of usage of these derivatives are being tracked on the state level by the National Institute of Drug Abuse Community Epidemiology Work Group [12]. Similarly, in the European Union, data from the Early Warning System have reported a steady increase in the number of police and forensic cases related to synthetic cathinones since 2009. The Michigan Morbidity and Mortality 2012 weekly report stated that 46 % of bath salt users presenting to emergency rooms had co-morbid mental illness, and 69 % had self-reported drug abuse [13].

In this present scenario, although few research exist on cathinone and its metabolic products [5, 14], there is still need for evaluation of chemical properties of cathinone and its chief metabolites. In this paper we reported conformational analysis, electronic structure, and thermodynamic properties of cathinone, norephedrine and norpseudoephedrine based on quantum chemical calculations and docking study. The molecular electrostatic potential surfaces (MEPS) of these molecules are also predicted. Based on the performed study, authors matched the probable metabolism pathway (Fig. 1) based on the work demonstrated by Brenneisen et al. [15]. With regard to the metabolic pathway published by Brenneisen et al., cathinone is metabolized to amino-alcohols by reduction of C-1 keto group, and two main metabolities are identified as norephedrine and norpseudoephedrine which are present in the (-) form with 1R configuration (Fig. 1 IV) [15].

Methodology

Potential energy surfaces were scanned, and all minima were optimized to find all possible conformers of cathinone, norephedrine, and norpseudoephedrine. All structures have been obtained using a relaxed dihedral angle scan to create a potential energy surface. Such obtained molecular structures were then optimized using two density functional theory's [16]: (a) B3LYP [17] and (b) MO26X [18] hybrid functional with 6-31G (d, p) basis sets. Previous studies [19] show that the basis set is enough for this type of calculation. All optimized surfaces (DFT) were calibrated by using Moller–Plesset second order calculations (MP2) [20]. The thermodynamic parameters of all compounds were calculated using statistical mechanics expressions.

Solvation free energies (ΔGsolv) were calculated at the DFT level with COSMO [21]. The ΔGsolv values were calculated in aqueous continuum ($\varepsilon = 78.39$), and the molecular cavities were built using the united atom for the Hartree–Fock (UAHF) procedure. In principle, the free energy surfaces are determined by rigorous combination of free energy perturbation/umbrella sampling approaches [22, 23]. These surfaces are very accurate, as they reflect non-equilibrium solvation. However, such calculations are very challenging when performed within the ab initio framework. Thus, a more practical, simplified approach has been applied. The relative free energies (ΔG) are determined as [24]:

$$\begin{aligned}\Delta G &= \Delta H_{gas}(298K) - T\Delta S - RT\ln(\omega) + \Delta\Delta G_{\text{solv}} \\ &\approx \Delta G_{\text{solv}}(298K) + \Delta\Delta G_{\text{solv}}\end{aligned} \quad (1)$$

In Eq. (1), ΔH_{gas}(298 K) represents enthalpy at 298 K, ΔS is the gas-phase entropy, ΔG_{gas}(298 K) is the Gibb's free energy at 298 K, and ΔG_{solv} is the relative free energy of solvation. The contribution of the RT ln (ω) term is zero, as the electronic degeneracy term, ω, for the singlet state is unity. $\Delta\Delta G_{\text{solv}}$ is solvation free energy calculated by COSMO model. The ΔG values are used to calculate the relative population of the various conformers of the molecules under study in aqueous medium.

Since the molecules are much more "floppy" in solution than in the gas phase, we have used another definition of

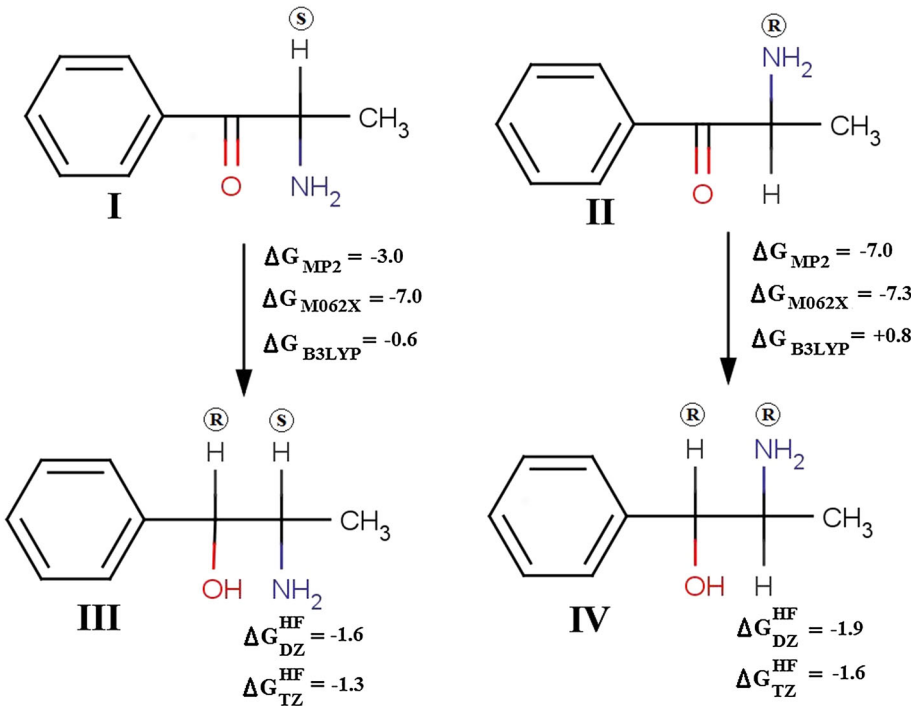

Fig. 1 Structures of the key urine metabolities of S-(−)-cathinone and R-(+)-cathinone. Where, (*I*) (−)-Cathinone, (*II*) (+)-Cathinone, (*III*) (−)-Norephedrine, and (*IV*) (−)-Norpseudoephedrine

free energy, (Δg_{flex}), to compare the intrinsic flexibility of different conformers, when embedded in aqueous medium. This is the practical implementation of the more general expression used by Warshel et al. [24, 25]. The Δg_{flex} could be expressed as

$$\Delta g_{\text{flex}} = \Delta E_{\text{solute}} + \Delta\text{ZPE} + \Delta\Delta G_{\text{solv}} - \alpha T\Delta S \quad (2)$$

where ΔE_{solute} and ΔZPE in Eq. (2) are the relative gas-phase energy separations and the zero-point energies of the various conformers. The scale factor α is usually taken as zero [25], and the expression (2) can be simplified as

$$\Delta g_{flex} = \Delta H_0^{gas} + \Delta\Delta G_{solv} \quad (3)$$

All terms in Eqs. (1) and (3) are available from the thermochemical analyses based on statistical mechanics expressions using the ideal gas, rigid rotator, and harmonic oscillator approximations [26], where ΔH_0^{gas} is zero-point energy available from frequency calculation. Natural bond orbital (NBO) analyses [27–29] have been also performed to corroborate the results as estimated from the MP2 and DFT calculations. ΔG calculations have been done by subtracting free Gibbs energy (from vibrational analysis) (Eq. 4) in gas phase.

$$\Delta G = G_{\text{Norephedrine/Norpseudoephedrine}} - (G_{\text{Cathinone}} + G_{H_2}) \quad (4)$$

IR spectra are also computed for all the studied molecules. All calculations were carried out using the GAUSSIAN 03 structure calculation software [30]. Molecular graphics were generated using the GAUSS VIEW visualization program [31].

Results and discussion

Cathinone

Cathinone has two conformers (Fig. 2I) connected by one transition state. The energy difference between two conformers is 1.6 kcal/mol for MP2 method, and 1.7 and 1.4 kcal/mol for DFT methods M062X and B3LYP, respectively. In case of MP2, the energetic barrier for the rotation is 5.1 kcal/mol. On the contrary, the barrier is higher for DFT calculations: 5.8 and 5.9 kcal/mol for M062X and B3LYP, respectively. The energy difference between two conformers *a* and *b* is lowered in water solutions and the values are as following: 1.3 kcal/mol, 1.5 kcal/mol, and 1.2 kcal/mol for MP2, M062X, and B3LYP, respectively. Calculation of the barrier high in solution shows that the obtained values are comparable with the gas-phase values for both DFT methods (Table 1). However, there is a difference of 1.2 kcal/mol between transition state in gas phase (5.0 kcal/mol) and solution (3.8 kcal/mol) for MP2 level. In Fig. 3, the energetic profile for cathinone calculated with 6-31G(d,p) basis set at the MP2 level is represented along with the energetic profile for DFT calculation. Molecular electrostatic potential (MEP) surfaces were generated to identify likely

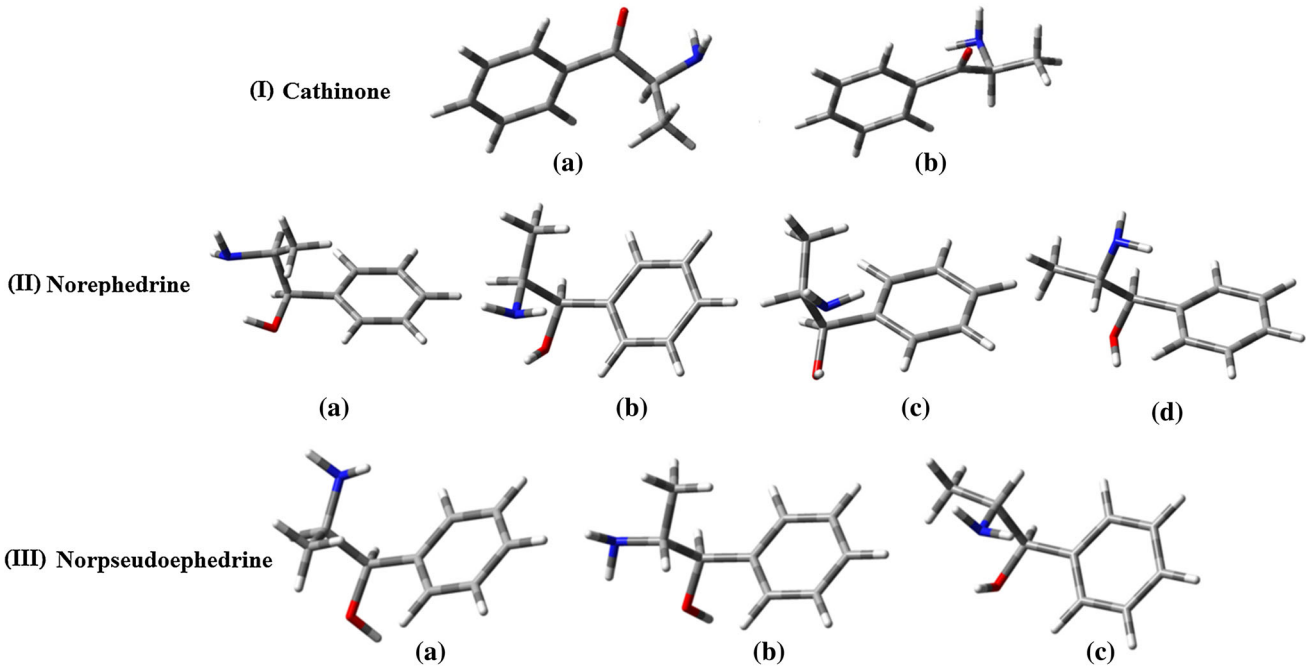

Fig. 2 Conformers of (*I*) cathinone, (*II*) norephedrine and (*III*) norpseudoephedrine

Table 1 Calculated energy for cathinone in gas and solution phase at 6-31G (d,p) basis set for DFT (M062X, B3LYP) and MP2 methods

Conformers	ΔH (kcal/mol)	μ [Debye]	g_{flex} (kcal/mol)
DFT (B3LYP)			
a	0.0	2.90	0.0
b	1.4	2.80	1.2
TS	5.9	2.27	5.6
DFT (M026X)			
a	0.0	2.74	0.0
b	1.7	2.68	1.5
TS	5.8	2.38	5.4
MP2			
a	0.0	3.35	0.0
b	1.6	3.23	1.3
TS	5.1	2.94	3.8

reaction sites and illustrated in Fig. 4a. Based on the analysis of Fig. 4a, it is clear that the most reactive sites are oxygen and nitrogen atoms; however, the geometry of the molecule allows for an attack on the most negative region of cathinone which is the carbonyl oxygen which leads to the formation of aminols, norephedrine, and norpseudoephedrine metabolites.

Norephedrine

Norephedirne has four conformers connected by five different transition states (Fig. 2II). Data calculated at the MP2 and DFT levels using 6-31G(d,p) basis set is presented in Table 2. The highest energy conformer is 4.3 kcal/mol above the lowest energy conformation for MP2 and; 4.7 and 4.1 kcal/mol for DFT (M062X and B3LYP functionals, respectively). The highest barrier connecting *b* and *d* conformers is 10.6, 9.9 and 8.8 kcal/mol for MP2, M062X and B3LYP methods, respectively. The lowest barrier is equal to 4.9 kcal/mol for MP2 and this transition state connects conformers *c* and *d*. Most interestingly, this trend is observed for both DFT calculations.

In solution, energies of conformers and their transition states have been lowered more significantly than in the gas phase. However, the energetic trend has been preserved, and the lowest energy conformer is the same for both gas phase and solution. In solution another low-energy conformer is identified. The highest barrier in solution is 9.9 kcal/mol for the b to d transition with the lowest barrier in solution being 3.9 kcal/mol for the transition from c to d. The energetic profile for transition between rotational conformers for gas phase and in solution for MP2 as well as DFT calculation is given in Fig. 5.

Populations calculated using Boltzmann distribution shows that the most populated conformations are *a* and *b* (Table 3) for both phases. In solution the population of *b* decreases, while the population of *a* and *c* increase from 42.3 to 48.6 % and from 1.3 to 2.5 %, respectively. Most importantly, solution phase provides a significant increase in population of d conformation which is nearly absent in gas phase.

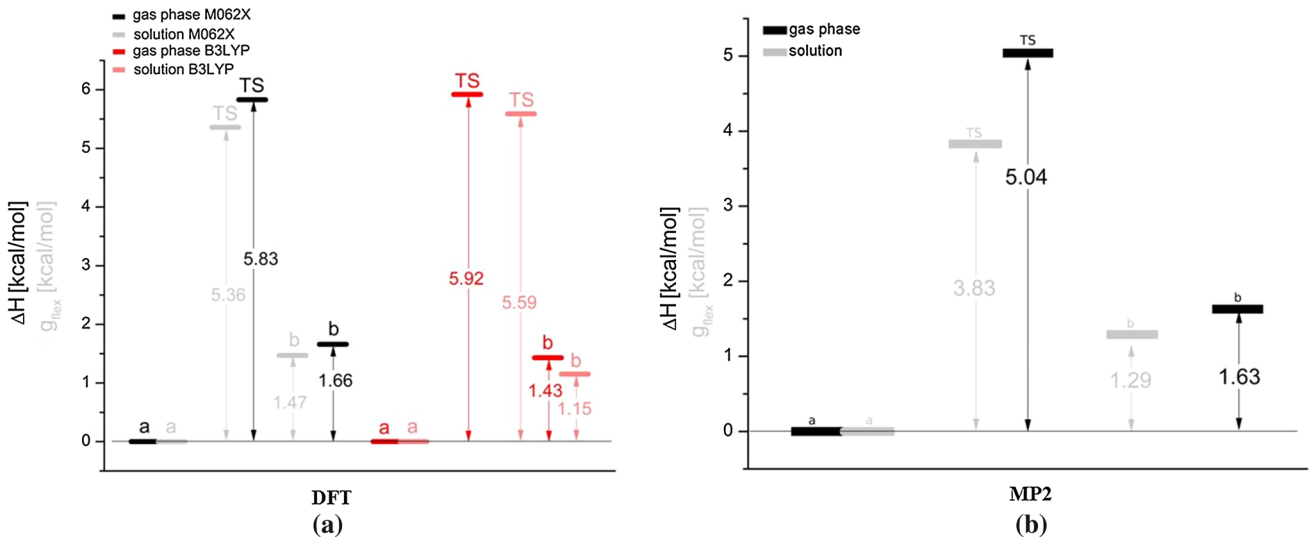

Fig. 3 Energetic profile of cathinone at DFT and MP2 level. Conformers of cathinone are indicated by label *a* and *b*. *TS* transition state

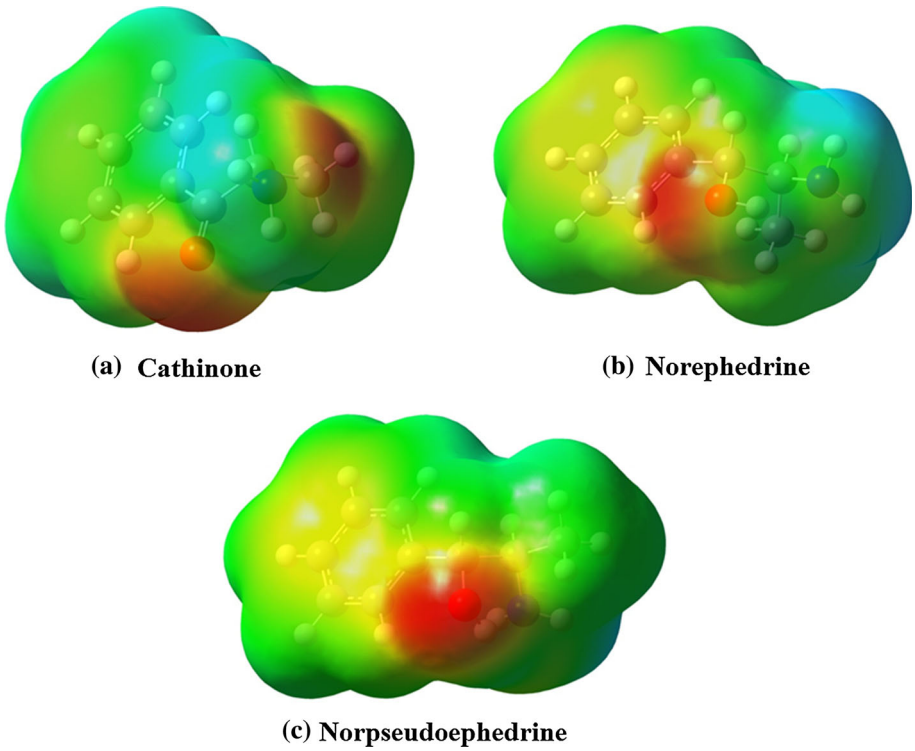

Fig. 4 MEP surface for the lowest conformer of **a** cathinone, **b** norephedrine, and **c** norpseudoephedrine. *Red* regions of the map are the most electron-rich regions of the molecule and *blue* regions are electron poor. Order of increasing electron density is *blue* < *green* < *yellow* < *orange* < *red* (Color figure online)

As with cathinone, data for norephedrine were calculated using different methods and the results are compared in Table 2. Calculations for both MP2 and DFT almost show an identical trend. The M062X results are more comparable with MP2 calculation than B3LYP. For MP2 calculation in solution energies of *a* and *b* conformers are equal. This trend is not visible for DFT calculations.

Calculated dipole moments for conformers vary from 2.19 to 3.37 D for MP2 and 1.04 to 3.14 D for M062X and from 1.04 to 3.12 D for B3LYP (Table 2). The trend is

Table 2 Calculated energy of norephedrine in gas and solution phase at 6-31G(d,p) basis set for DFT (M062X, B3LYP) and MP2 methods

Conformer	ΔH (kcal/mol)	μ [Debye]	g_{flex} (kcal/mol)
DFT (B3LYP)			
a	0.5	3.12	0.5
b	0.0	2.98	0.0
c	1.9	2.55	1.6
d	4.1	1.04	3.3
b↔c	7.6	2.37	6.8
b↔d	8.8	1.02	8.3
c↔d	4.4	0.67	3.6
a↔b	5.8	3.43	5.1
a↔c	6.4	2.52	6.3
DFT (M026X)			
a	0.3	3.14	0.4
b	0.0	2.96	0.0
c	2.3	2.62	1.9
d	4.7	1.04	3.8
b↔c	8.9	2.46	8.5
b↔d	9.9	1.07	9.5
c↔d	4.9	0.68	4.2
a↔b	6.8	3.27	6.3
a↔c	7.7	2.60	7.5
MP2			
a	0.2	3.37	0.0
b	0.0	3.15	0.0
c	2.2	2.90	1.8
d	4.3	2.19	3.2
b↔c	8.9	2.75	8.2
b↔d	10.6	1.35	9.9
c↔d	4.9	0.73	3.9
a↔b	6.9	3.37	6.4
a↔c	7.2	2.90	6.8

Table 3 Populations of norephedrine and norpseudoephedrine in gas phase and solution

Phase	Gas		Solution	
Conformer	ΔH (kcal/mol)	%	ΔH (kcal/mol)	%
Norephedrine				
a	0.2	42.3	0.0	48.6
b	0.0	56.3	0.0	48.6
c	2.2	1.3	1.8	2.5
d	4.3	0.1	3.2	0.3
Norpseudoephedrine				
a	2.4	1.8	2.2	2.1
b	1.8	4.8	1.1	14.6
c	0.0	93.4	0.00	83.3

preserved for all methods which is consistent with the calculated MEP surface. The MEP surface calculations show that the most active site of norephedrine molecule is located around the oxygen atom. However, the site is less pronounced than in case of cathinone and the region around the nitrogen atom is not active (Fig. 4b).

Norpseudoephedrine

Norpseudoephedrine has three conformers connected by two transition states (Fig. 2III). The energetic profile for norpseudoephedrine at MP2 level of theory is shown in Fig. 6. In solution, conformers' energy is decreased more than in the gas phase. The highest energy conformer is located 2.4 kcal/mol (2.2 kcal/mol) above the lowest energy conformation for gas (and solution phase) (Table 4). The *a* conformer is the lowest energy conformer for B3LYP calculation while *b* and *a* are the highest ones

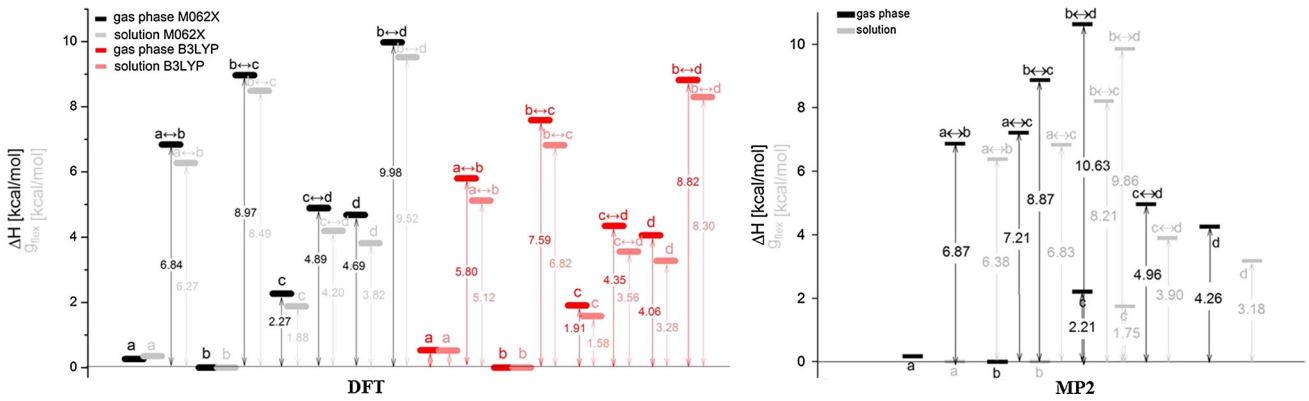

Fig. 5 Energetic profile of norephedrine calculated at MP2 level. Conformers of norephedrine are indicated by label *a*, *b*, *c* and *d*. *TS* transition state

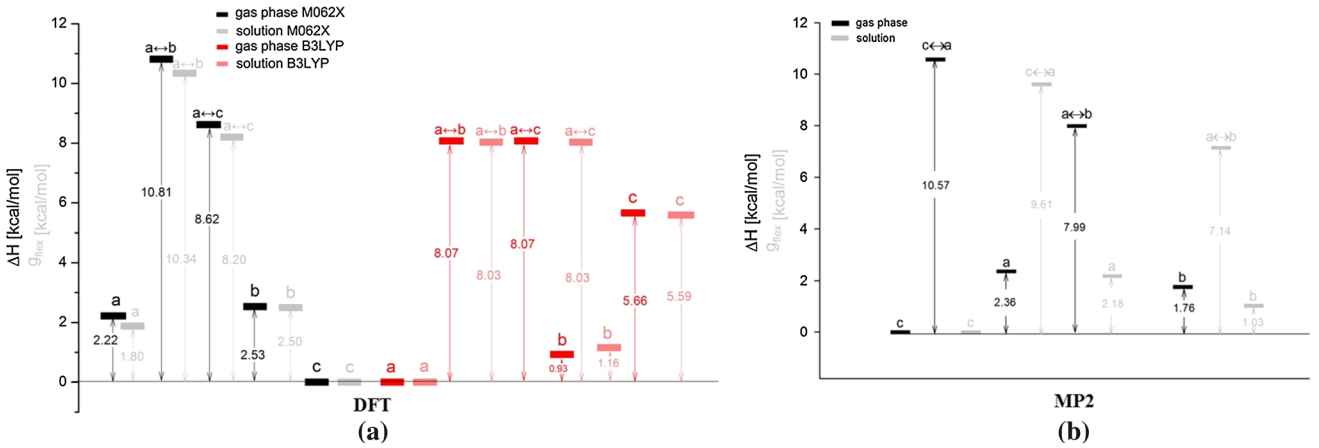

Fig. 6 Energetic profile of norpseudoephedrine calculated at MP2 level. Conformers of norephedrine are indicated by label *a*, *b* and *c*. *TS* transition state

Table 4 Calculated energies for norpseudoephedrine in gas and solution phase at 6-31G(d,p) basis set for DFT (M062X, B3LYP) and MP2 methods

Conformer	ΔH (kcal/mol)	μ [Debye]	g_{flex} (kcal/mol)
DFT (B3LYP)			
a	0.0	1.17	0.00
b	0.9	0.96	1.2
c	5.7	0.36	5.6
a↔c	8.1	0.32	8.0
a↔b	8.1	0.32	8.0
DFT (M026X)			
a	2.2	1.20	1.9
b	2.5	1.01	2.50
c	0.0	2.91	0.00
a↔c	8.6	0.34	8.2
a↔b	10.8	0.37	10.3
MP2			
a	2.4	1.21	2.2
b	1.8	1.47	1.0
c	0.0	3.14	0.00
a↔c	10.6	0.40	7.1
a↔b	8.0	0.42	9.6

for M062X and MP2, respectively. The highest energy barrier is 10.6 kcal/mol as calculated at the MP2 level for a to c transition. The highest energy for transition state for M062X method is 10.8 kcal/mol as transition occurs from a to b. The energy barrier calculated using B3LYP level of theory is 8.1 kcal/mol for both a to c and a to b transitions. Interestingly, these conformers are characterized by the same dipole moment but different shape of molecules. The energetic profile for DFT level of theory is also illustrated in Fig. 6.

The lowest energy conformer (*c*) is the most populated in both gas and solution phase (Table 3). Population analysis reveals that the population of conformer *b* increases in solution from 4.75 to 14.63 %. On the contrary, the population of conformer *c* decreases in solution from 93.50 to 83.27 %. Analysis of norpseudoephedrine's MEPS shows (Fig. 4c) the most active site for norpseudoephedrine is located on the oxygen atom. It is interesting to point out that the active site potency is decreasing in the following order: norpseudoephedrine > norephedrine > cathinone. Again, like norephedrine, the nitrogen region is inactive for norpseudoephedrine.

IR spectra

Based on the ΔG calculation, high electronegativity of oxygen atom and hybridization of C=O bond facilitate attack on this bond and addition of hydrogen atom in reaction pathway. Calculated ΔG value from cathinone to norephedrine and norpseudoephedrine are illustrated in Fig. 1. Analysis of calculated and experimental IR spectra (Table 5) shows that method that repeats the most experimental spectra is MP2 for cathinone and its metabolites [32–34]. The MP2 method repeats both trend and position of harmonic frequencies and a scaling factor [35] is applied for MP2/6-31G (d, p) only for better comparison between experimental and computed IR peaks for all molecules. Comparing experimental and calculated IR graphs, we found that norephedrine and norpseudoephedrine main peaks are almost at the same position. A notable change for C=C ring vibration can be noticed for cathinone because of influence of substitution in metabolites.

Table 5 Comparison between experimental and calculated characteristic vibrations of cathinone, norephedrine and norpseudoephedrine employing IR spectrum

Cathinone			Norephedrine		Norpseudoephedrine		Method
Vibration	Experimental (cm^{-1})[a]	Calculated (cm^{-1})	Experimental (cm^{-1})[b]	Calculated (cm^{-1})	Experimental (cm^{-1})[c]	Calculated (cm^{-1})	
C=O stretching	1667	1743 (1692*)	–	–	–	–	MP2
		1761					M06-2X
		1835					B3LYP
O–H waving	–	–	~640	648 (629*)	~705	665 (645*)	MP2
				609		648	M06-2X
				632		310	B3LYP
O–H stretching	–	–	~3650	3728 (3619*)	~3700	3710 (3602*)	MP2
				3762		3793	M06-2X
				3657		3818	B3LYP
N–H asymmetric stretching	~3500	3644 (3538*)	~3560	3670 (3563*)	~3600	3674 (3567*)	MP2
		3593		3623		3633	M06-2X
		3548		3584		3583	B3LYP
C–H stretching	2512	3129 (3038*)	~2900	3015 (2927*)	2878	3081 (2992*)	MP2
		3089		2981		3030	M06-2X
		3051		2920		2939	B3LYP
C=C ring vibrating	~1560–1590	1655–1676 (1607–1627*)	~500–650	480–630 (466–611*)	~700	628–633 (609–614*)	MP2
		1696.41		415–523		622–648	M06-2X
		1634–1654		517–632		555–650	B3LYP
H ring + CH_3 vibrating	2512–2877	3129–3287 (3038–3192*)	~3000–3200	3130–3295 (3039–3199)	~3100–3359	3128–3290 (3037–3262*)	MP2
		3089–3234		3072–3236		3068–3230	M06-2X
		3051–3221		33,050–3226		3047–3207	B3LYP

[a,b,c] refers to reference numbers 31, 32 and 33, respectively

* Refers to the reference number 34

Docking study and bond population analysis of protein-molecule complex

Docking approach

Protein preparation The X-ray structure of Drosophila dopamine transporter bound to psychostimulant D-amphetamine was taken from the Protein Databank (PDB ID: 4XP9) and prepared for docking using the following procedure:

(1) Bound D-amphetamine is removed from the protein; modified protein and removed D-amphetamine are saved as separate files in.pdb format
(2) The waters of crystallization were removed from the protein structure, and
(3) Hydrogen atoms were added to the structure and the entire molecule was subjected to optimization employing Autodock Tools 1.5.6 [36].

Ligand preparation Least energy conformers of cathinone, ephedrine and norpseudoephedrine for the mentioned three quantum mechanical methods are taken as ligand molecule by saving in.pdb format. So, total nine ligands are considered for docking.

Docking First to validate the accuracy of applied docking method, D-amphetamine was docked in the protein to check whether it is binding completely to the previous binding sites as described in the PDB employing PatchDock software [37]. The input parameters were included in the PDB coordinate files for prepared protein 4XP9 and D-amphetamine molecule with setting clustering RMSD to 1.5. Analyzing the output of the docking, the benzene ring of D-amphetamine is involved in π–π interaction with Phe43C and 2 strong hydrogen bonding with Ala44c and Asp46c with the free amine group of molecule. This suggests that the same residues are interacting with D-amphetamine when it is present in the protein as co-crystalised ligand. After validating the methods, each studied molecules optimized using all three methods were docked in the protein following mentioned parameters. Scoring function that considers both geometric fit and atomic desolvation energy [38] was used to evaluate each candidate transformation. Based on the atomic contact energy or desolvation energy, docking score, and approximate interface area of the complex, best docking solution was selected for further refinement and rescoring analysis by FireDock (Fast Interaction REfinement in molecular DOCKing) algorithm. PatchDock is aimed at finding docking transformations that yield good molecular shape complementarity. The main reason behind PatchDock's high efficiency is its fast transformational search, which is driven by local feature matching, rather than brute force searching of the six-dimensional transformation space.

In case of cathinone, three conformers from three optimized methods are bound to the protein in the same orientation. However, in case of norephedrine and norpseudoephedrine, conformer obtained from M062X had shown completely opposite orientation in the active site of protein from other two conformers obtained from B3LYP and MP2 methods. Cathinone and norpseudoephedrine surrounded in the active pocket consisted of nine amino acid residues as Phe43, Ser421, Phe319, Phe325, Gly425, Val120, Tyr124, Ser320, and Asp46 of C chain of the protein. However, norephedrine active pocket consists of three more amino acid residues (Ala44, Ser422 and Gly322) along with mentioned nine residues. Docking studies revealed all the conformers showed good binding energy towards the target protein and the result highly comparable with the D-amphetamine (see Table 6). The docked conformations are illustrated in Fig. 7. As, the interaction of the studied conformers with the amino acid residues and binding energies are almost comparable for the studied molecules, further bond population analysis of complexes had been performed to interpret the stabilization energies of different interaction and identify why potencies are vary from one molecule to another [39].

Table 6 Docked desolvation energy of the studied molecules in different optimization methods

Molecules	Desolvation energy (kcal/mol)
Amphetamine	−6.3
Cathinone-B3LYP	−6.2
Cathinone-MO62X	−6.4
Cathinone-MP2	−6.2
Norephedrine-B3LYP	−6.0
Norephedrine-MO62X	−6.1
Norephedrine-MP2	−6.0
Norpseudoephedrine-B3LYP	−6.4
Norpseudoephedrine-MO62X	−5.9
Norpseudoephedrine-MP2	−5.9

Bond population analysis of protein–molecule complexes

Bond population analysis for individual compounds is illustrated in Supplementary file along with the 2D contour diagrams (Figure S1) of NBO. The NBO analysis of interacting amino acid residues and ligands (low-energy conformers of studied molecules optimized through the mentioned methods) has been performed, followed by docking studies. Cathinone conformers obtained from the optimization methods show similar pattern of results. On the contrary, norephedrine and norpseudoephedrine results obtained are method dependent and MP2 and B3LYP data differs from those obtained using M062X optimized molecular geometries.

The NBO analysis of cathinone suggests that there are two lone pairs localized on oxygen atoms overlapping $sp^{0.82}$ hybrid and p-orbital. One lone pair is localized on nitrogen atom with $sp^{3.81}$ hybrid. Natural orbital charges localized on oxygen and nitrogen atoms are −0.595 and −0.909, respectively. In case of cathinone, the stabilizing energies between interacting residues and cathinone are below 0.9 kcal/mol. On the contrary, the highest self-stabilizing energy for cathinone's bonding orbital C=C and antibonding C–O* is 19.9 kcal/mol. However, the value significantly changes for C–O and C=C* to 3.9 kcal/mol.

The C–O bond in norephedrine is represented by the presence of electrons $sp^{3.92}$ and $sp^{3.90}$ hybrid on C and $sp^{2.16}$ and $sp^{2.36}$ on hybrid O atom for M062X and MP2/B3LYP, respectively, comparing with the stand alone molecule $sp^{3.83}$. The changes have been represented in Figure (number) (norephedrine-NBO-M06 and norephedrine-NBO-B3LYP). The stabilizing energy for C=C/C–O* is 1.9 and 1.2 kcal/mol for M062X and MP2/B3LYP, respectively. It changes for C–O/C = C* to 1.7 and 1.9 kcal/mol for M062X and MP2/B3LYP, respectively.

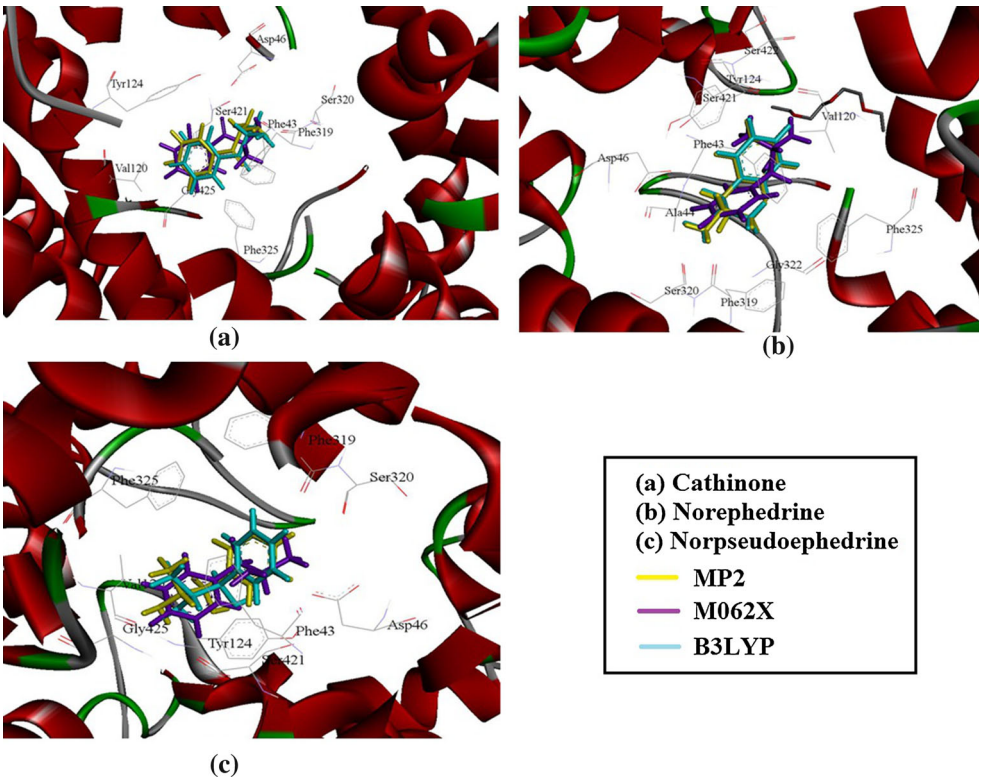

Fig. 7 Docked binding modes for the Cathinone, Norephedrine and Norpseudoephedrine

Charges localized on oxygen and nitrogen atoms are presented in Table 7 for all optimization methods. Two significant stabilizing energies are identified between lone pair localized on oxygen atom of SER320 and C–H group from benzene ring of 1.5 and 10.2 kcal/mol between N atom of ligand and C–H* of VAL120 for M062X optimization process. In case of MP2/B3LYP calculations, stabilizing energies between SER320 C–O and ligand's N–H* is 2.7 kcal/mol, SER320 lone pair O atom and ligand's N–H* is 4.1 kcal/mol; and weak stabilizing energy between ligand's N–H and C–O* of SER320 is 1.1 kcal/mol. The highest stabilizing energy identified between lone pair O atom of PHE319 and O–H* of ligand's is 10.3 kcal/mol.

From the NBO calculations, the C–O bond of norpseudoephedrine is represented by the presence of electrons on $sp^{3.99}$ and $sp^{3.93}$ hybrid C (M062X and MP2/B3LYP, respectively) and $sp^{2.32}$ and $sp^{2.37}$ hybrid O (M062X and MP2/B3LYP, respectively). The computed stabilizing energies between C=C and C–O* are 1.6 kcal/mol for the M062X and 4.5 kcal/mol for MP2/B3LYP calculations. Again, the stabilizing energy between C–O and C=C* is equal to 1.76 for M062X method and 1.7 kcal/mol for the MP2/B3LYP calculations. Comparing all the studied molecules, norpseudoephedrine has the highest values of stabilizing energies for interaction between ligand and amino acid residues. The lone pairs of electron localized on oxygen atom (both pairs) and nitrogen atom take part in stabilizing whole ligand and hydrogen bonding with residues. The computed NBO charges localized on oxygen and nitrogen atoms are presented in Table 7 for all considered optimization methods. Calculations using M062X approach reveal six high stabilization energies among norpseudoephedrine and amino acid residues. They are described below:

(1) C–H (Benzene ring) of PHE325 and lone pair O of ligand is 14.2 kcal/mol,
(2) Lone pair of O atom of PHE319 and C–H* of ligand is 12.2 kcal/mol,
(3) Lone pair of O atom of PHE45 and N–H* of ligand is 3.2 kcal/mol,
(4) First and second lone pair of O atom of ALA44 and C–H* of ligand are 4.2 and 3.6 kcal/mol, respectively,

Table 7 NBO charges on oxygen and nitrogen atoms of cathinone and its metabolites inside active pocket of protein

Atom	Molecules	M062X	MP2/B3LYP
Oxygen	Cathinone	−0.595	−0.595
	Norephedrine	−0.778	−0.803
	Norpseudoephedrine	−0.820	−0.814
Nitrogen	Cathinone	−0.909	−0.909
	Norephedrine	−0.953	−0.922
	Norpseudoephedrine	−0.989	−0.931

(5) Lone pair of O atom of TYR124 and N–H* of ligand is 15.6 kcal/mol.

In case of MP2/B3LYP calculations, there are six high stabilization energies between amino acid residues and ligand. The measured stabilization energies between ligand and amino acid residues are as follows:

(1) The C–O fragment of TYR124 and O–H* of ligand is 1.1 kcal/mol,
(2) First and second lone pair of O atom of TYR124 and O–H* of ligand are 19.6 and 27.2 kcal/mol, respectively
(3) Lone pair of O atom of SER421 and N–H* of ligand is 4.9 kcal/mol,
(4) Lone pair of O atom of ligand and C–H* of SER421 is 14.5 kcal/mol, and
(5) Internal stabilization energy between lone pair of O atom and N–H* of ligand is 8.6 kcal/mol.

The cumulative docking study followed by NBO calculation of studied ligands in the active site of the amino acid residues of proteins strongly support the experimental studies why potency of the compounds follows the order: norpseudoephedrine > norephedrine > cathinone through stabilizing energies and interaction of these ligands in the studied protein [39]. The 2D graph of NBO electrostatic potential (ESP) of cathinone and its metabolites in active site of protein is presented in Figure S2 in Supplementary file.

Conclusions

The comprehensive study carried out for three title molecules revealed that the applied DFT functionals provide reliable energy trend for ground states but not for a transition state. Cathinone has two active regions located on the oxygen and nitrogen atoms. The oxygen atom is the most reactive site of the molecule which explains the formation of the metabolites of cathinone–norephedrine and norpseudoephedrine. Norephedrine has four low-energy conformers with the differences between lowest and highest energy conformers of about 4 kcal/mol for both MP2 and DFT methods and a weakly active region located on the oxygen atom. Norpseudoephedrine has three low-energy conformers. The M062X calculations provide the same energy trend as MP2 for the ground state but not for transition state structures. However, the energies predicted at the B3LYP level are not comparable with the results of MP2 calculations neither for the ground nor transition state structures.

Active regions for norpseudoephedrine and norephedrine located on the oxygen atoms indicate that there is a possibility for conversion of harmless compounds and probably facilitate removal of these metabolities from the body. Based on the Boltzmann distribution calculations, cathinone and norephedrine moieties in solution have two abundant conformers populated at about 50 % each. The calculated IR spectra for both cathinone and its derivatives are similar to experimental ones thus one is certain that the calculated molecules correspond accurately to the measured species. The conjecture is further substantiated by the MP2 and DFT calculations followed by NBO analyses and supported by ΔG calculations.

Docking study followed by NBO calculations of the amino acid residues and ligand complex explore stabilizing energy of the studied molecules with the interacting proteins along with the reason behind the difference in potency for cathinone's metabolites. The NBO result suggested that the lone pairs located on oxygen and nitrogen atoms involved in high stabilizing interactions between ligand and amino acid residues are stabilized through formation of hydrogen bonding for norpseudoephedrine. The highest stabilizing energy is identified between lone pair located on oxygen atom of TYR124 and O–H group of norpseudoephedrine making it the most stable and potent molecule in active pocket of studied protein 4XP9 among the considered molecules. This strongly supports and explains the results of experimental studies [39]. Again, NBO study of the complex revealed that the internal stabilization energy of C=C (benzene ring) to C–O* and C–O to C=C* (benzene ring) are the highest for cathinone and the smallest for its metabolites which makes them active and potent molecule in the body.

Acknowledgments We would like to thank the Wroclaw Supercomputing and Networking Center for the generous allotment of computer time and the Mississippi Center for Supercomputing Research. S. K. and J. L. thank the National Science Foundation (NSF/CREST HRD-1547754, and EPSCoR (Award #: 362492-190200-01\NSFEPS-0903787) for financial support.

References

1. Kassie F, Darroudi F, Kundi M et al (2001) Khat (*Catha edulis*) consumption causes genotoxic effects in humans. Int J Cancer 92:329–332
2. Baumann MH, Ayestas MA, Partilla JS et al (2011) The designer methcathinone analogs, mephedrone and methylone, are

substrates for monoamine transporters in brain tissue. Neuropsychopharmacology 37:1192–1203. doi:10.1038/npp.2011.304
3. Hillebrand J, Olszewski D, Sedefov R (2010) Legal highs on the Internet. Subst Use Misuse 45:330–340
4. Kalix P (1985) The khat alkaloid (−) cathinone acts like amphetamine on physiological catecholamine stores. NIDA Res Monogr Ser 55:286
5. Al-Motarreb A, Baker K, Broadley KJ (2002) Khat: pharmacological and medical aspects and its social use in Yemen. Phyther Res 16:403–413
6. Kalix P (1992) Cathinone, a natural amphetamine. Pharmacol Toxicol 70:77–86
7. Al-Motarreb A, Al-Habori M, Broadley KJ (2010) Khat chewing, cardiovascular diseases and other internal medical problems: the current situation and directions for future research. J Ethnopharmacol 132:540–548
8. Suwalsky M, Zambrano P, Mennickent S et al (2011) Effects of phenylpropanolamine (PPA) on in vitro human erythrocyte membranes and molecular models. Biochem Biophys Res Commun 406:320–325. doi:10.1016/j.bbrc.2011.01.117
9. Macdonald F (1997) Dictionary of pharmacological agents. CRC Press, Boca Raton
10. Bonano JS, Glennon RA, De Felice LJ et al (2014) Abuse-related and abuse-limiting effects of methcathinone and the synthetic "bath salts" cathinone analogs methylenedioxypyrovalerone (MDPV), methylone and mephedrone on intracranial self-stimulation in rats. Psychopharmacology 231:199–207. doi:10.1007/s00213-013-3223-5
11. https://aapcc.s3.amazonaws.com/files/library/Bath_Salts_Data_for_Website_1.09.2013.pdf (2012) American Association of Poison Control Centers, Bath Salt Data
12. Forrester MB, Kleinschmidt K, Schwarz E, Young A (2011) Synthetic cannabinoid exposures reported to Texas poison centers. J Addict Dis 30:351–358. doi:10.1080/10550887.2011.609807
13. Report MW (2011) Recreational water illness and injury prevention week—estimated burden of acute otitis externa—United States, 2003–2007. Mortality 60:2009–2011
14. Dal Cason TA, Young R, Glennon RA (1997) Cathinone: an investigation of several N-alkyl and methylenedioxy-substituted analogs. Pharmacol Biochem Behav 58:1109–1116
15. Brenneisen R, Geisshusler S, Schorno X (1986) Metabolism of cathinone to (−)-norephedrine and (−)-norpseudoephedrine. J Pharm Pharmacol 38:298–300
16. Parr RG, Yang W (1989) Density-functional theory of atoms and molecules. Density Funct, Theory Atoms Mol
17. Becke AD (1993) Density-functional thermochemistry. III. The role of exact exchange. J Chem Phys 98:5648–5652
18. Zhao Y, Truhlar DG (2007) The M06 suite of density functionals for main group thermochemistry, thermochemical kinetics, noncovalent interactions, excited states, and transition elements: two new functionals and systematic testing of four M06-class functionals and 12 other function. Theor Chem Acc 120:215–241. doi:10.1007/s00214-007-0310-x
19. Kolodziejczyk W, Jodkowski J, Holmes TM, Hill GA (2013) Conformational analysis of flephedrone using quantum mechanical models. J Mol Model 19:1451–1458. doi:10.1007/s00894-012-1673-z
20. Moller C, Plesset MS (1943) Note on an approximation treatment for many-electron systems. Phys Rev 46:618. doi:10.1103/PhysRev.56.841.2
21. Barone V, Cossi M (1998) Quantum calculation of molecular energies and energy gradients in solution by a conductor solvent model. J Phys Chem A 102:1995–2001
22. Hwang J-K, King G, Creighton S, Warshel A (1988) Simulation of free energy relationships and dynamics of SN2 reactions in aqueous solution. J Am Chem Soc 110:5297–5311
23. Warshel A (1991) No Title. Computer modeling of chemical reactions in enzims solutions
24. Florián J, Warshel A (1998) Phosphate ester hydrolysis in aqueous solution: associative versus dissociative mechanisms. J Phys Chem B 102:719–734
25. Florián J, Štrajbl M, Warshel A (1998) Conformational flexibility of phosphate, phosphonate, and phosphorothioate methyl esters in aqueous solution. J Am Chem Soc 120:7959–7966
26. Davidson N (1962) No Title. Stat. Mech
27. Reed AE, Weinhold F (1983) Natural bond orbital analysis of near-Hartree–Fock water dimer. J Chem Phys 78:4066–4073
28. Badenhoop JK, Weinhold F (1997) Natural steric analysis: ab initio van der Waals radii of atoms and ions. J Chem Phys 107:5422–5432
29. Badenhoop JK, Weinhold F (1997) Natural bond orbital analysis of steric interactions. J Chem Phys 107:5406–5421
30. Frisch MJ, Trucks GW, Schlegel HB, et al (2009) Gaussian 2009
31. Commercial Molecular Graphics Software (2005) GAUSSVIEW 2005
32. http://www.swgdrug.org/Monographs/cathinone.pdf
33. http://webbook.nist.gov/cgi/cbook.cgi?ID=C492411&Mask=80
34. http://www.spectra-analysis.com/infraredspectra/controlled.htm
35. Alecu IM, Zheng J, Zhao Y, Truhlar DG (2010) Computational thermochemistry: scale factor databases and scale factors for vibrational frequencies obtained from electronic model chemistries. J Chem Theory Comput 6:2872–2887. doi:10.1021/ct100326h
36. http://autodock.scripps.edu/resources/references
37. http://bioinfo3d.cs.tau.ac.il/PatchDock/
38. Zhang C, Vasmatzis G, Cornette JL, DeLisi C (1997) Determination of atomic desolvation energies from the structures of crystallized proteins. J Mol Biol 267:707–726. doi:10.1006/jmbi.1996.0859
39. Eisenberg MS, Maher TJ, Silverman HI (1987) A comparison of the effects of phenylpropanolamine, d-amphetamine and d-norpseudoephedrine on open-field locomotion and food intake in the rat. Appetite 9:31–37. doi:10.1016/0195-6663(87)90051-1